

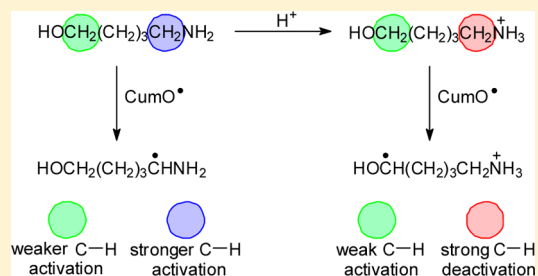
Fine Control over Site and Substrate Selectivity in Hydrogen Atom Transfer-Based Functionalization of Aliphatic C–H Bonds

Michela Salamone, Giulia Carboni, and Massimo Bietti*

Dipartimento di Scienze e Tecnologie Chimiche, Università “Tor Vergata”, Via della Ricerca Scientifica, 1 I-00133 Rome, Italy

S Supporting Information

ABSTRACT: The selective functionalization of unactivated aliphatic C–H bonds over intrinsically more reactive ones represents an ongoing challenge of synthetic chemistry. Here we show that in hydrogen atom transfer (HAT) from the aliphatic C–H bonds of alkane, ether, alcohol, amide, and amine substrates to the cumyloxy radical (CumO•) fine control over site and substrate selectivity is achieved by means of acid–base interactions. Protonation of the amines and metal ion binding to amines and amides strongly deactivates the C–H bonds of these substrates toward HAT to CumO•, providing a powerful method for selective functionalization of unactivated or intrinsically less reactive C–H bonds. With 5-amino-1-pentanol, site-selectivity has been drastically changed through protonation of the strongly activating NH₂ group, with HAT that shifts to the C–H bonds that are adjacent to the OH group. In the intermolecular selectivity studies, trifluoroacetic acid, Mg(ClO₄)₂, and LiClO₄ have been employed in an orthogonal fashion for selective functionalization of alkane, ether, alcohol, and amide (or amine) substrates in the presence of an amine (or amide) one. Ca(ClO₄)₂, that promotes deactivation of amines and amides by Ca²⁺ binding, offers, moreover, the opportunity to selectively functionalize the C–H bonds of alkane, ether, and alcohol substrates in the presence of both amines and amides.



INTRODUCTION

C–H bond functionalization is currently a mainstream topic of synthetic chemistry and one of the most investigated approaches to develop new synthetic methodology.^{1–4} Functionalization of aliphatic C–H bonds generally proceeds at the most reactive center of an organic substrate. Accordingly, the development of selective functionalization procedures that are able to overcome the inherent or innate reactivity of different C–H bonds, i.e., procedures that occur selectively at an unactivated aliphatic C–H bond over a functional group or a C–H bond that is activated by an adjacent functional group, represents one of the major challenges of modern synthetic organic chemistry. Among the available procedures, the use of bulky transition-metal-based catalysts that are able to discriminate between different C–H bonds on the basis of steric accessibility is emerging as a convenient strategy for selective functionalization of primary and secondary unactivated aliphatic C–H bonds^{5,6} and of methane over alkane and cycloalkane substrates.^{7,8} Great interest has been also attracted by directing group strategies, where site-selectivity is achieved through binding of a transition-metal catalyst or an organic activator group to a substrate functionality.^{9–11} The need for covalent installation and removal of the directing group generally represents, however, a major drawback of this strategy. An alternative approach is provided by enzymatic and biomimetic C–H bond oxidations, where substrate positioning via specific noncovalent interactions and steric effects can promote site-selective C–H functionalization.^{12–20} Availability, stability, and substrate specificity of the enzymes

and metal-based catalysts limit, however, the applicability of this approach.

Deactivating polar effects can be also employed to control site-selectivity. In aliphatic C–H bond functionalization procedures based on hydrogen atom transfer (HAT) to radical or radical-like species, the main factor that governs HAT reactivity is represented by bond strengths, but other factors such as steric, stereoelectronic, strain release, and polar effects have also been shown to play an important role.^{21–23} As a consequence of the electrophilic nature of the majority of the hydrogen atom abstraction reagents employed,²⁴ functionalization generally occurs at the more electron-rich C–H bonds (i.e., the C–H bonds that are α to a heteroatom in substrates such as amines, amides, alcohols, and ethers or C–H bonds that are remote from an electron-withdrawing group).^{3,17c,19c,25–28} Along this line, remote, undirected aliphatic C–H functionalization of amine substrates has been successfully achieved following deactivation of the proximal C–H bonds via protonation or Lewis acid complexation at the nitrogen center.^{29–32} These acid–base interactions convert an activating electron-donating group into a strong electron-withdrawing and deactivating group, inverting the polarity of the adjacent C–H bonds and decreasing their reactivity toward electrophilic hydrogen atom abstracting reagents.^{21,28} Most importantly, in these reactions site-selectivity is achieved by

Received: July 29, 2016

Published: September 12, 2016

means of cheap and easily available Brønsted and Lewis acidic additives.

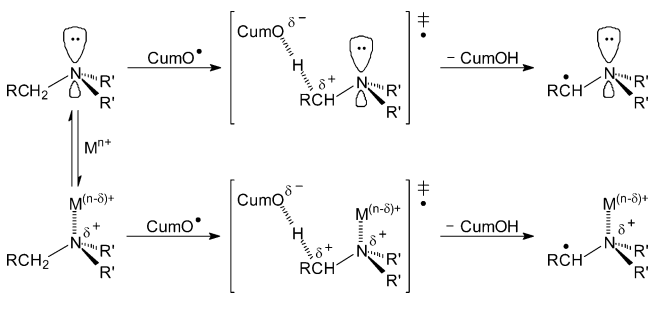
Within this framework, recent studies have provided a quantitative evaluation of the α -C–H bond deactivation of basic substrates toward a genuine and electrophilic HAT reagent such as the cumyloxyl radical ($\text{PhC}(\text{CH}_3)_2\text{O}^\bullet$, CumO^\bullet) determined by acid–base interactions. Transient kinetic and computational studies have shown that in acetonitrile solution protonation or Mg^{2+} complexation leads to a >4-order of magnitude decrease in the rate constant for HAT (k_{H}) from the α -C–H bonds of aliphatic amines to CumO^\bullet .^{33–35} Strong deactivating effects have been also observed in the presence of Ca^{2+} ,³⁶ whereas significantly weaker effects have been observed when the same reactions have been carried out in the presence of Li^+ , quantified on the basis of a ~ 2 -fold decrease in k_{H} .³³

C–H bond deactivation has been also observed in the reactions of CumO^\bullet with tertiary alkanamides following addition of alkali and alkaline earth-metal ions.³⁷ Strong C–H deactivation has been observed in acetonitrile solution after addition of Li^+ and Ca^{2+} , where in particular the latter metal ion has been observed to promote deactivation of up to four substrate equivalents. A significantly weaker deactivation has been instead observed in the presence of Mg^{2+} , quantified on the basis of a ~ 3 -fold decrease in k_{H} .

With aliphatic ethers, no significant effect on k_{H} for HAT to CumO^\bullet has been observed after addition of a Brønsted acid such as trifluoroacetic acid (TFA).^{34b} A ≤ 3 -fold decrease in k_{H} has been instead measured when the corresponding reactions have been carried out in the presence of Li^+ or Mg^{2+} ,³³ in line with the relatively weaker Lewis basicity of ethers as compared to amines and amides.

This behavior has been explained in terms of protonation or metal ion (M^{n+}) binding to the basic center of these substrates. These interactions increase the bond dissociation enthalpy of the α -C–H bonds,^{35,38} decreasing the electron density of these bonds and of the product radical, leading to a destabilization of the HAT transition state and to an overall α -C–H bond deactivation toward CumO^\bullet (Scheme 1, showing the effect of metal ion binding on HAT from a tertiary alkylamine to CumO^\bullet).^{21,33,34}

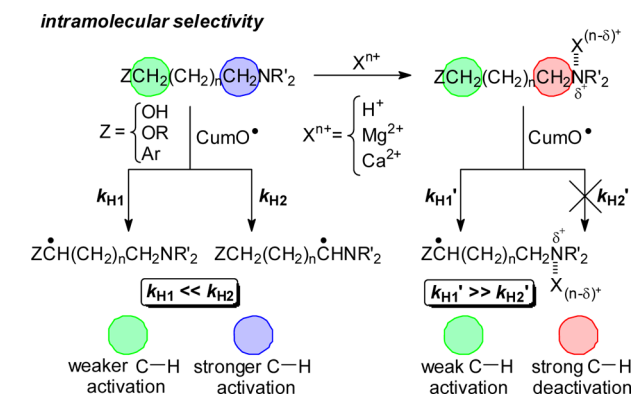
Scheme 1



Taken together, these results clearly show that C–H deactivation can be modulated varying the Brønsted or Lewis basicity of the substrate as well as the nature and strength of the acid, allowing for careful control over the HAT reactivity of basic substrates toward alkoxy (and, more generally, electrophilic) radicals. Comparison between the results obtained with the different substrates shows that deactivation of C–H bonds that are proximal to amine or amide functionalities toward HAT to electrophilic radicals can be achieved through

protonation or proper selection of the added alkali or alkaline earth-metal ion. Most importantly, these results suggest that this approach can provide a method for site-selective C–H bond functionalization of substrates bearing functionalities characterized by different basicities (intramolecular selectivity, Scheme 2) or for selective functionalization of an aliphatic or a

Scheme 2



weakly basic substrate (alkane, ether, alcohol) in the presence of a more basic and intrinsically more reactive amine and/or amide substrate (intermolecular selectivity, Scheme 3). These possibilities appear of great interest in the framework of the development of synthetically useful selective C–H functionalization procedures based on HAT to electrophilic hydrogen atom abstracting species.

Within this framework, in order to address these issues and to obtain information on the effect of Brønsted and Lewis acids on the intermolecular HAT selectivity, detailed transient kinetic studies on the reactions of CumO^\bullet with a variety of selected substrate couples and triads have been carried out. The following substrates have been chosen for this purpose: cyclooctane (COT), dibenzylether (DBE), tetrahydrofuran (THF), cyclohexanol (CHXOH), *N,N*-dimethylacetamide (DMA), cyclohexylamine (CHXNH₂), triethylamine (TEA), and 1,2,2,6,6-pentamethylpiperidine (PMP).

RESULTS AND DISCUSSION

In these studies, CumO^\bullet has been generated by 355 nm laser flash photolysis of acetonitrile solutions containing the parent dicumyl peroxide, and the second-order HAT rate constants (k_{H}) have been obtained from the slope of the observed rate constant (k_{obs}) vs [substrate] plots, where in turn the k_{obs} values have been measured following the decay of the CumO^\bullet visible absorption band ($\lambda_{\text{max}} = 485 \text{ nm}$)³⁹ at the different substrate concentrations. Most importantly, this laser flash photolysis approach can provide direct and reliable information on the HAT process, without complications generally associated with indirect information extracted from catalytic procedures, where multiple steps are involved and overfunctionalization can be observed, often leading to mass balance problems, and partially masking the intrinsic HAT selectivity.

It is well-established that with the chosen substrates, HAT to alkoxy radicals predominantly occurs from the α -C–H bonds of ethers, alcohols, and amines⁴⁰ and from the *N*-methyl groups of DMA.⁴¹ The k_{H} values measured in acetonitrile solution at $T = 25 \text{ }^\circ\text{C}$, for reaction of CumO^\bullet with the hydrogen atom donor substrates employed in this study are collected in Table 1.

Scheme 3

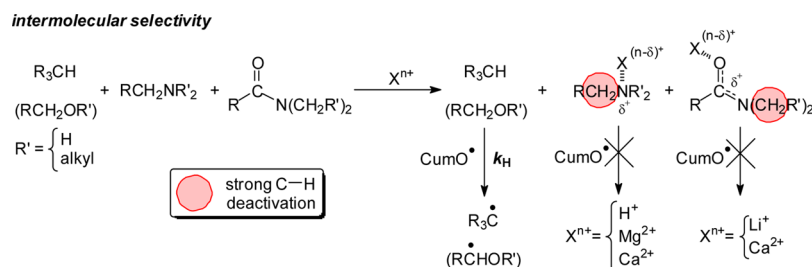


Table 1. Second-Order Rate Constants (k_H) for Reaction of CumO• with Different Hydrogen Atom Donor Substrates Measured in Acetonitrile at $T = 25\text{ }^\circ\text{C}$

substrate	k_H ($M^{-1} s^{-1}$) ^a
cyclooctane (COT)	$(3.2 \pm 0.1) \times 10^6$ ^b
tetrahydrofuran (THF)	$(5.8 \pm 0.1) \times 10^6$ ^c
dibenzyl ether (DBE)	$(5.62 \pm 0.02) \times 10^6$ ^b
cyclohexanol (CHXOH)	$(2.66 \pm 0.05) \times 10^6$ ^b
<i>N,N</i> -dimethylacetamide (DMA)	$(1.47 \pm 0.02) \times 10^6$ ^b
cyclohexylamine (CHXNH ₂)	$(2.1 \pm 0.1) \times 10^7$ ^b
triethylamine (TEA)	$(2.0 \pm 0.1) \times 10^8$ ^d
1,2,2,6,6-pentamethylpiperidine (PMP)	$(1.70 \pm 0.02) \times 10^8$ ^d

^aThe given values are the average of at least two independent kinetic experiments. ^bThis work. ^cRef 42. ^dRef 40d.

TFA has been used as Brønsted acid for quantitative protonation of the amine substrates, while LiClO₄, Mg(ClO₄)₂, and Ca(ClO₄)₂ have been used for metal-ion binding to the amine and/or amide substrates. Substrate couples and acid additives have been chosen in such a way as to determine selective C–H bond deactivation of one substrate via protonation (amine) or metal ion complexation (amine or amide) over a second hydrocarbon, ether, alcohol, amide, or amine substrate. The HAT reactivity of substrate triads has

been studied exclusively in the presence of Ca(ClO₄)₂, and the triads have been chosen in such a way as to determine selective deactivation of two substrates via metal ion complexation (amine and amide), over a third hydrocarbon or other substrate.

Kinetic studies have been complemented by product analysis of the reactions of CumO• with COT and DBE, where the intermolecular selectivity has been studied carrying out the reactions in the presence of an amine substrate such as PMP and of a stoichiometric amount of TFA. In these studies, CumO• has been generated by visible light irradiation of dichloromethane solutions containing cumyl alcohol (CumOH), (diacetoxyiodo)benzene (DIB), and iodine (I₂).⁴³

Information on the effect of TFA on the intramolecular HAT selectivity has been obtained through a detailed transient kinetic study in acetonitrile solution on the reactions of CumO• with 5-amino-1-pentanol (APOH), with comparison to the corresponding reactions with pentane (PentH), 1-pentanol (PentOH), and 1-aminopentane (PentNH₂).

Intermolecular Selectivity. Starting from the study of the reactions of CumO• with COT, a representative saturated hydrocarbon substrate, the following k_H value has been measured in acetonitrile, from the slope of the k_{obs} vs [COT] plot: $k_H = (3.2 \pm 0.1) \times 10^6 M^{-1} s^{-1}$ (Figure 1a,b, black circles). The intercept of this plot mostly reflects the

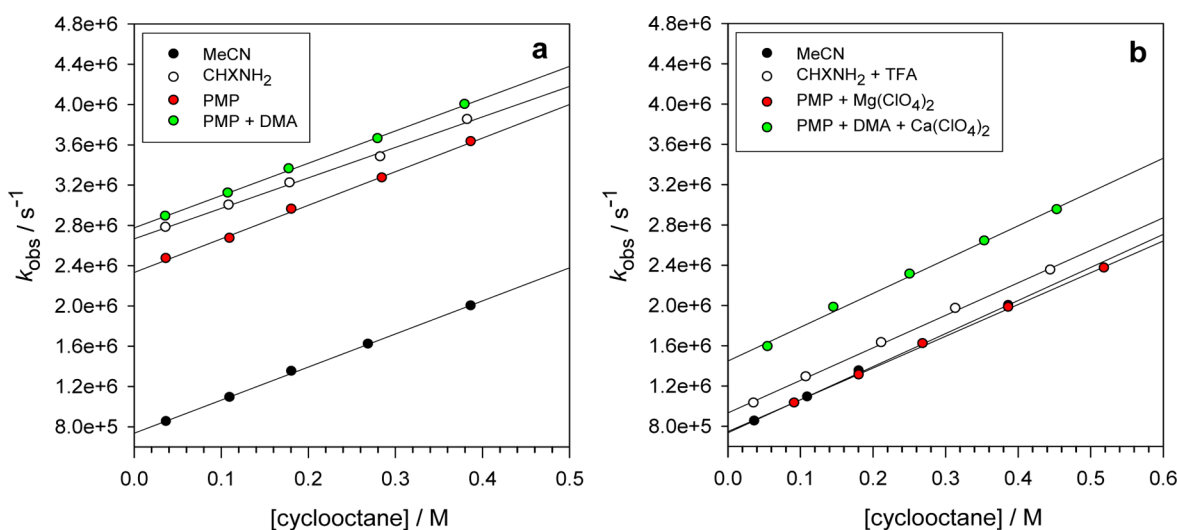


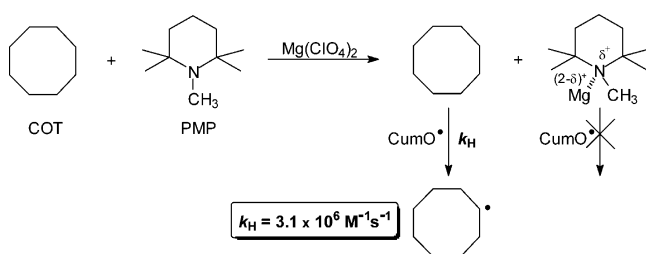
Figure 1. Plots of k_{obs} vs [cyclooctane] for reaction with the cumyloxyl radical (CumO•). (a) In acetonitrile (black circles) and in acetonitrile containing: (i) 0.1 M CHXNH₂ (white circles); (ii) 0.01 M PMP (red circles); (iii) 0.01 M PMP and 0.2 M DMA (green circles). (b) In acetonitrile (black circles) and in acetonitrile containing: (i) 0.1 M CHXNH₂ and 0.1 M TFA (white circles); (ii) 0.01 M PMP and 0.01 M Mg(ClO₄)₂ (red circles); (iii) 0.01 M PMP, 0.2 M DMA, and 0.2 M Ca(ClO₄)₂ (green circles). From the linear regression analysis: in acetonitrile, $k_H = (3.2 \pm 0.1) \times 10^6 M^{-1} s^{-1}$. (a) (i) $k_H = (3.05 \pm 0.06) \times 10^6 M^{-1} s^{-1}$; (ii) $k_H = (3.2 \pm 0.1) \times 10^6 M^{-1} s^{-1}$; (iii) $k_H = (3.30 \pm 0.05) \times 10^6 M^{-1} s^{-1}$. (b) (i) $k_H = (3.19 \pm 0.05) \times 10^6 M^{-1} s^{-1}$; (ii) $k_H = (3.1 \pm 0.1) \times 10^6 M^{-1} s^{-1}$; (iii) $k_H = (3.40 \pm 0.04) \times 10^6 M^{-1} s^{-1}$. The different intercepts observed in graph (b) reflect the effect of the acid additive on the CumO• β -scission rate constant.^{33,37a}

contribution from C–CH₃ β -scission in CumO[•].^{39a} Negligible effects on k_H have been observed after addition of 0.1 M TFA, 0.6 M LiClO₄, or 0.2 M Ca(ClO₄)₂ (Supporting Information (SI), Figure S1). No significant effect on k_H has been also observed when the reaction has been studied in the presence of (i) 0.1 M CHXNH₂ (Figure 1a, white circles), (ii) 0.01 M PMP (red circles), and (iii) 0.01 M PMP and 0.2 M DMA (green circles). As compared to acetonitrile, the significantly higher values of the intercepts for the k_{obs} vs [COT] plots reflect the kinetic contribution of HAT from the α -C–H bonds of the added amines (CHXNH₂ and PMP) and from the *N*-methyl groups of DMA, clearly indicating that under these conditions, competitive HAT from COT and from the added amine and amide substrates occurs.

Almost identical k_H values have been measured when the same reactions have been carried out in the presence of Brønsted and Lewis acid additives, namely (i) 0.1 M CHXNH₂ and 0.1 M TFA (Figure 1b, white circles), (ii) 0.01 M PMP and 0.01 Mg(ClO₄)₂ (red circles), and (iii) 0.01 M PMP, 0.2 M DMA and 0.2 M Ca(ClO₄)₂ (green circles), where, however, a sharp decrease in the intercepts of the k_{obs} vs [COT] plots has been observed.⁴⁴ In particular, the different intercepts observed in Figure 1b reflect the effect of the acidic additive on the CumO[•] β -scission rate constant (see for comparison the pertinent k_{obs} vs [COT] plots displayed in Figure S1).^{33,37a}

The almost identical slopes observed for the k_{obs} vs [COT] plots under these diverse experimental conditions and, most importantly, the sharp decrease in intercept clearly show that protonation of CHXNH₂ by TFA, Mg²⁺ binding to PMP, and Ca²⁺ binding to PMP, and DMA can promote strong deactivation of the C–H bonds of these substrates, with HAT to CumO[•] that now exclusively occurs from COT, despite of the fact that the α -C–H bonds of CHXNH₂ and PMP are significantly more reactive toward CumO[•] ($k_H = 2.1 \times 10^7$ and $1.7 \times 10^8 \text{ M}^{-1} \text{ s}^{-1}$, respectively), while the α -C–H bonds of DMA display a comparable reactivity ($k_H = 1.47 \times 10^6 \text{ M}^{-1} \text{ s}^{-1}$). A representative example is displayed in Scheme 4,

Scheme 4



where, according to the plot displayed in Figure 1a,b (red circles) for the reaction of CumO[•] with COT and PMP, the effect of added Mg²⁺ on the intermolecular HAT selectivity is shown.

Additional experiments where the concentration of COT has been initially varied, followed by a concentration variation of other hydrogen atom donor substrates [(i) PMP, (ii) DMA and PMP, (iii) DMA, (iv) CHXNH₂], by addition of a Lewis or Brønsted acid [(i) Mg(ClO₄)₂, (ii) Ca(ClO₄)₂, (iii) LiClO₄, (iv) TFA], and by a second variation in [COT], fully support this mechanistic picture (Figures 2a,b, S3, and S4, respectively).

Competitive HAT from the C–H bonds of the different substrates is initially observed, evidenced by the change in slope of the k_{obs} vs [substrate] plots that accompanies addition of the

different substrates (points 1–2 and points 1–3 in Figure 2a,b, respectively). Successive addition of the Brønsted or Lewis acid (marked with # in Figure 2a,b, and indicative of the addition of Mg(ClO₄)₂ and Ca(ClO₄)₂, respectively) deactivates the basic amine and/or amide substrates by protonation or metal ion binding, as clearly shown by the sharp decrease in k_{obs} observed following addition. The increase in reactivity observed in the last concentration range reflects selective HAT from COT to CumO[•], as evidenced by the very similar slopes (i.e., k_H values) measured in the first and last region of the k_{obs} vs [substrate] plots (points 3 and 4 in Figure 2a,b, respectively). A representative example is shown in Scheme 5, where, according to the plots displayed in Figure 2a, the effect of sequential addition of COT, PMP, Mg(ClO₄)₂, and COT on the reaction with CumO[•] is shown.

Product studies on the reaction of CumO[•] with COT have been also carried out following visible light irradiation (30–120 min) of argon saturated dichloromethane solutions containing COT (0.4–1.0 M), CumOH (0.10 M), DIB (0.22 M), and I₂ (0.11 M). Formation of cyclooctyl acetate (COTOAc) and acetophenone (AcPh) as the exclusive reaction products has been observed. Both COTOAc and AcPh increase with increasing irradiation time, whereas an increase in substrate concentration from 0.4 to 1.0 M leads to a 3-fold increase in the COTOAc/AcPh ratio. These results can be accounted for on the basis of the competitive pathways described in Scheme 6, where AcPh derives from C–CH₃ β -scission in the first formed CumO[•] (path a),^{39a} whereas the formation of COTOAc can be explained in terms of the acetolysis of cyclooctyl iodide, formed following HAT from COT to CumO[•] (path b) and reaction of the cyclooctyl radical thus formed with I₂ (path c), clearly indicating that COTOAc represents the exclusive product deriving from the HAT pathway. On the basis of this picture, an increase in [COT] will increase the relative importance of the bimolecular HAT pathway over the unimolecular β -scission one.

By carrying out the reaction in the presence of PMP (0.05–0.10 M) and of a stoichiometric amount of TFA, the same product distribution has been observed, and quantitative recovery of PMP has been obtained after workup. This result is again indicative of the strong deactivation toward HAT of the α -C–H bonds of PMP determined by protonation, in full agreement with the mechanistic picture discussed above.

Moving to representative ether substrates such as THF and DBE, the following k_H values have been measured in acetonitrile after reaction with CumO[•]: $k_H = (5.8 \pm 0.1) \times 10^6$ and $(5.62 \pm 0.02) \times 10^6 \text{ M}^{-1} \text{ s}^{-1}$, respectively. Negligible effects on k_H have been observed after addition of 0.1 M TFA^{34b} or 0.2 M Ca(ClO₄)₂ (Figure S5), whereas a ≤ 3 -fold decrease in k_H has been measured after addition of 1.0 M LiClO₄ or Mg(ClO₄)₂.³³ No significant effect on k_H has been also observed when the reaction with THF has been studied in the presence of (a) 0.1 M CHXNH₂ and TFA, (b) 0.2 M PMP and TFA, (c) 0.2 M TEA and TFA, and (d) 0.01 M PMP and Mg(ClO₄)₂ (Figure S6) and when the reaction with DBE has been studied in the presence of (a) 0.2 M PMP and TFA, (b) 0.2 M TEA and TFA, (c) 0.5 M TEA and TFA, and (d) 0.01 M PMP, 0.2 M DMA, and 0.2 M Ca(ClO₄)₂ (Figure S7). These results clearly indicate that also under these conditions, protonation of the amine substrates (CHXNH₂, PMP and TEA) by TFA, Mg²⁺ binding to PMP, and Ca²⁺ binding to PMP, and DMA promotes strong deactivation of the C–H

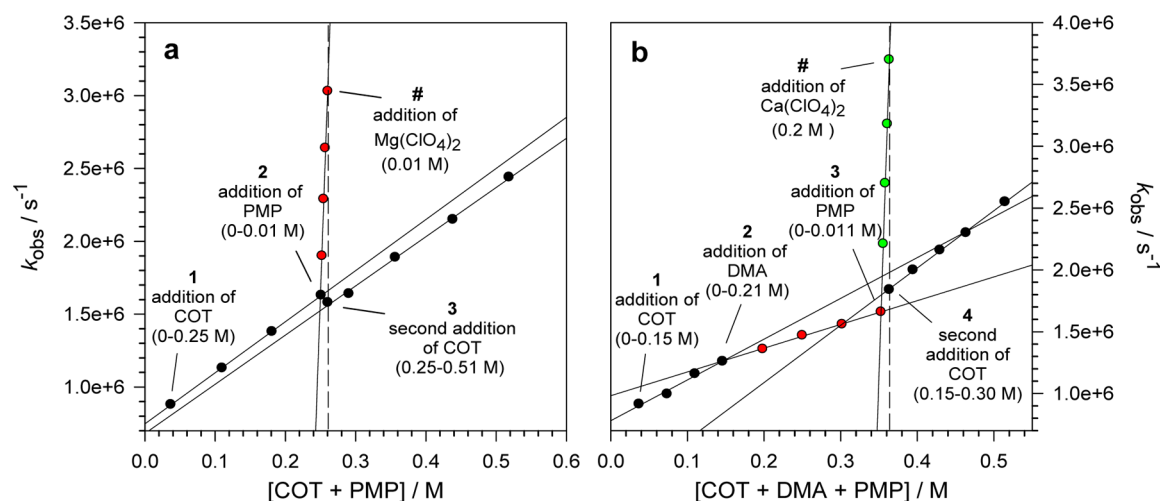
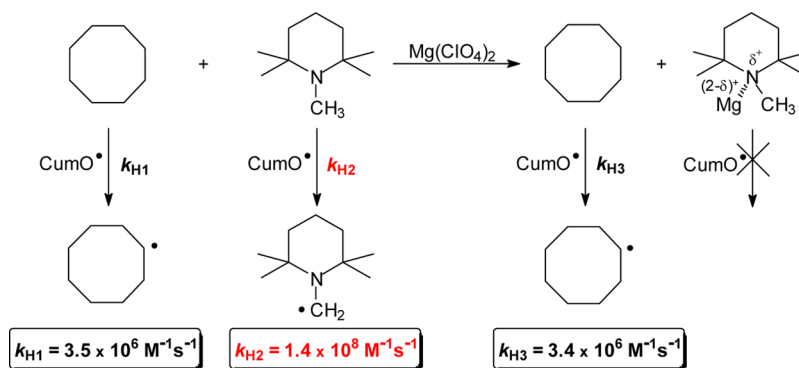
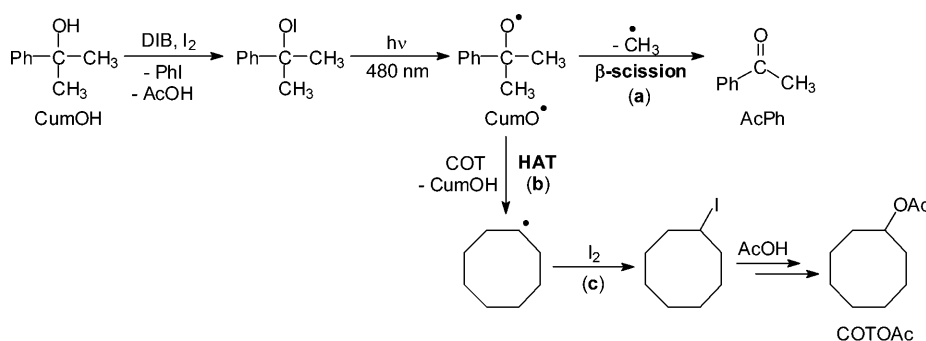


Figure 2. Plots of k_{obs} vs [substrate] for reaction with the cumyloxy radical (CumO^\bullet) in acetonitrile, following sequential addition of: (a) COT (black circles), PMP (red circles), $\text{Mg}(\text{ClO}_4)_2$ and COT (black circles); (b) COT (black circles), DMA (red circles), PMP (green circles), $\text{Ca}(\text{ClO}_4)_2$ and COT (black circles). From the linear regression analysis: (a) $k_{\text{H1}} = 3.51 \times 10^6 \text{ M}^{-1} \text{ s}^{-1}$, $k_{\text{H2}} = 1.36 \times 10^8 \text{ M}^{-1} \text{ s}^{-1}$, $k_{\text{H3}} = 3.38 \times 10^6 \text{ M}^{-1} \text{ s}^{-1}$. (b) $k_{\text{H1}} = 3.30 \times 10^6 \text{ M}^{-1} \text{ s}^{-1}$, $k_{\text{H2}} = 1.92 \times 10^6 \text{ M}^{-1} \text{ s}^{-1}$, $k_{\text{H3}} = 1.87 \times 10^8 \text{ M}^{-1} \text{ s}^{-1}$, $k_{\text{H4}} = 4.64 \times 10^6 \text{ M}^{-1} \text{ s}^{-1}$. In (b), the shift in the intercept of the first and fourth plot (black circles) reflects the effect of $\text{Ca}(\text{ClO}_4)_2$ on the CumO^\bullet β -scission rate constant.^{37a}

Scheme 5



Scheme 6



bonds of these substrates, with HAT to CumO^\bullet that selectively occurs from THF or DBE.

The same reactivity pattern has been observed in experiments where the concentration of THF or DBE has been initially varied, followed by a sequential concentration variation of other hydrogen atom donor substrates, by addition of a Brønsted or Lewis acid, and by a second variation in the concentration of the ether substrate (for THF: (i) TEA and TFA (Figure 3a); for DBE: (i) DMA, PMP and $\text{Ca}(\text{ClO}_4)_2$ (Figure 3b); (ii) PMP and TFA (Figure S8)) and in experiments where, starting from an acetonitrile solution

containing the Lewis acid, the concentration of the ether substrate has been initially varied, followed by a concentration variation of other hydrogen atom donor substrates and by a second variation in the concentration of the ether substrate (for THF, starting from an acetonitrile solution containing 0.6 M LiClO_4 : DMA (Figure S9); for DBE, starting from an acetonitrile solution containing 0.2 M $\text{Ca}(\text{ClO}_4)_2$: DMA and PMP (Figure S10).

When the sequential concentration variation of the hydrogen atom donors (points 1–2 and 1–3 in Figure 3a,b, respectively) has been followed by addition of the Brønsted or Lewis acid

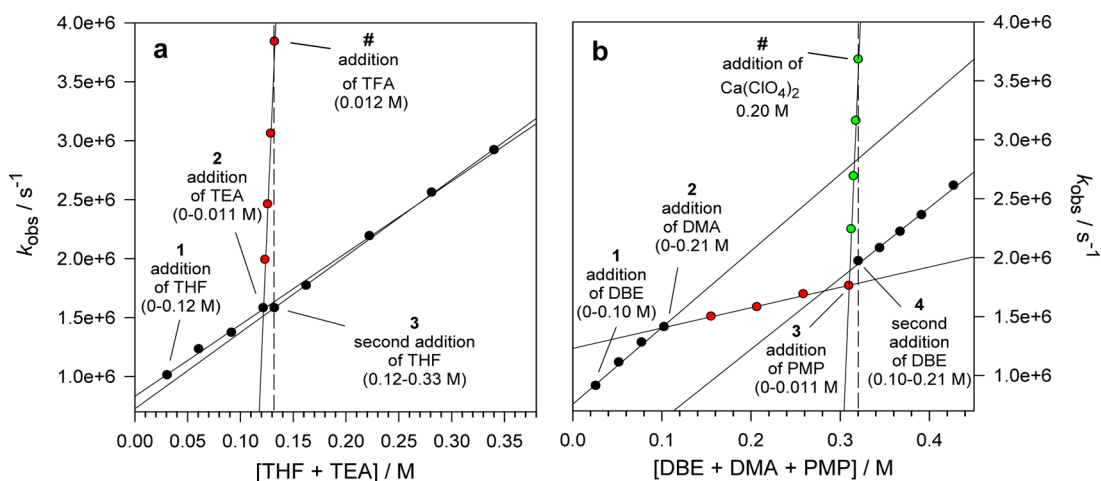
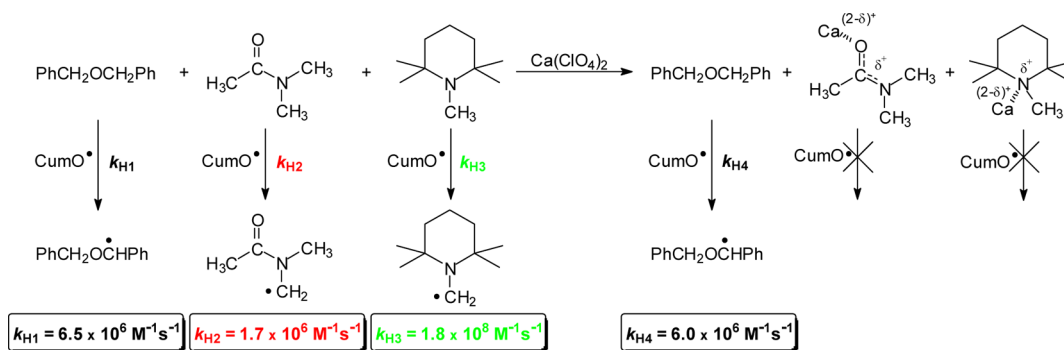


Figure 3. Plots of k_{obs} vs [substrate] for reaction with the cumyloxy radical (CumO^\bullet) in acetonitrile, following sequential addition of: (a) THF (black circles), TEA (red circles), TFA and THF (black circles); (b) DBE (black circles), DMA (red circles), PMP (green circles), $\text{Ca}(\text{ClO}_4)_2$ and DBE (black circles). From the linear regression analysis: (a) $k_{\text{H1}} = 6.08 \times 10^6 \text{ M}^{-1} \text{ s}^{-1}$; $k_{\text{H2}} = 2.10 \times 10^8 \text{ M}^{-1} \text{ s}^{-1}$; $k_{\text{H3}} = 6.48 \times 10^6 \text{ M}^{-1} \text{ s}^{-1}$. (b) $k_{\text{H1}} = 6.50 \times 10^6 \text{ M}^{-1} \text{ s}^{-1}$; $k_{\text{H2}} = 1.72 \times 10^6 \text{ M}^{-1} \text{ s}^{-1}$; $k_{\text{H3}} = 1.80 \times 10^8 \text{ M}^{-1} \text{ s}^{-1}$; $k_{\text{H4}} = 6.01 \times 10^6 \text{ M}^{-1} \text{ s}^{-1}$. In (b), the shift in the intercept of the first and fourth plot (black circles) reflects the effect of $\text{Ca}(\text{ClO}_4)_2$ on the CumO^\bullet β -scission rate constant.^{37a}

Scheme 7



(marked with # in Figure 3a,b, and indicative of the addition of TFA and $\text{Ca}(\text{ClO}_4)_2$, respectively), competitive HAT from the C–H bonds of the different substrates has been initially observed. Protonation deactivates the amine substrates while Ca^{2+} binding deactivates both the amine and amide substrates, as clearly shown by the sharp decrease in k_{obs} observed following addition of TFA and $\text{Ca}(\text{ClO}_4)_2$. The increase in reactivity observed in the last concentration range (points 3 and 4 in Figure 3a,b, respectively) reflects in both cases selective HAT from THF or DBE to CumO^\bullet . A representative example is shown in Scheme 7, where, according to the plots displayed in Figure 3b, the effect of sequential addition of DBE, DMA, PMP, $\text{Ca}(\text{ClO}_4)_2$, and DBE on the reaction with CumO^\bullet is shown.

When the sequential concentration variation of the hydrogen atom donors has been carried out on an acetonitrile solution containing the Lewis acid, the linear increase in reactivity observed in the first and last concentration range reflects selective HAT from the ether substrate to CumO^\bullet , as evidenced by the very similar slopes measured in these regions for the k_{obs} vs [substrate] plots (Figures S9 and S10). The negligible effect on reactivity observed after addition of DMA (in the reaction carried out in the presence of LiClO_4 : Figure S9) or after addition of DMA and PMP (in the reaction carried out in the presence of $\text{Ca}(\text{ClO}_4)_2$: Figure S10) is instead

indicative of the strong C–H bond deactivation of these substrates determined by metal ion binding.

Product studies on the reaction of CumO^\bullet with DBE (for details see the SI) have shown the formation of benzaldehyde and benzyl alcohol as the exclusive products deriving from HAT from the benzylic C–H bonds of this substrate, accompanied by acetophenone (AcPh) formed following CumO^\bullet β -scission. When the reaction with CumO^\bullet has been carried out in the presence of 0.10 M PMP and 0.10 M TFA, formation of the same products and quantitative recovery of PMP has been observed, providing an additional example of the selective deactivation toward HAT of the C–H bonds of a more basic and intrinsically more reactive amine substrate over an ether substrate determined by protonation.

Additional experiments on the reactions of CumO^\bullet with selected substrate couples have shown moreover that selective C–H bond deactivation of an amine (TEA or PMP) or amide (DMA) substrate over an alcohol (CHXOH), amide (DMA), or amine (PMP) one can be successfully achieved following addition of TFA, $\text{Mg}(\text{ClO}_4)_2$, or LiClO_4 . The k_{obs} vs [substrate] plots showing selective deactivation of DMA over CHXOH and of DMA over PMP by LiClO_4 addition; of PMP over DMA, TEA over DMA, and TEA over CHXOH by TFA addition; of PMP over DMA, and PMP over CHXOH by $\text{Mg}(\text{ClO}_4)_2$ addition, are displayed in Figures S11–S17, respectively. The results obtained in the present study on the effect of Brønsted



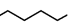

and Lewis acidic additives on the intermolecular HAT selectivity for reactions of CumO^\bullet with hydrogen atom donor substrate couples and triads are summarized in Table 2.

Table 2. Effect of Brønsted and Lewis Acidic Additives on the Intermolecular HAT Selectivity for Reactions of CumO^\bullet with Hydrogen Atom Donor Substrate Couples and Triads

additive	strong C–H bond deactivation for	selective HAT from
H^+	amine	alkane, ether (alcohol), amide
Mg^{2+}	amine	alkane, ether (alcohol), amide
Li^+	amide	alkane, ether (alcohol), amine
Ca^{2+}	amine and amide	alkane, ether (alcohol)

Intramolecular Selectivity. In order to obtain information on the role of acid–base interactions on the intramolecular HAT selectivity, the effect of TFA on the reaction of CumO^\bullet with 5-amino-1-pentanol (APOH) has been investigated by laser flash photolysis. As a matter of comparison the corresponding reactions of CumO^\bullet with pentane (PentH), 1-pentanol (PentOH), and 1-aminopentane (PentNH₂) have been also studied. The k_{H} values thus obtained are collected in Table 3. The pertinent k_{obs} vs [substrate] plots are displayed in Figure S18.

Table 3. Second-Order Rate Constants (k_{H} , $\text{M}^{-1} \text{s}^{-1}$) for Reaction of CumO^\bullet with Pentane Derivatives Measured in Acetonitrile at $T = 25^\circ \text{C}$

				
	PentH	PentOH	PentNH ₂	APOH
k_{H}	$(3.1 \pm 0.1) \times 10^5$	$(1.46 \pm 0.07) \times 10^6$	$(1.55 \pm 0.02) \times 10^7$	$(1.58 \pm 0.02) \times 10^7$
$k_{\text{H}}(\text{rel})$	1	4.7	50	51

By taking into account that the C–H bonds of unactivated methyl groups display an extremely low reactivity toward alkoxy radicals ($k_{\text{H}}(\text{CH}_3) \leq 1.3 \times 10^4 \text{ M}^{-1} \text{ s}^{-1}$ per methyl group),⁴⁵ it can be reasonably concluded that the k_{H} value measured for reaction of CumO^\bullet with PentH ($k_{\text{H}} = 3.1 \times 10^5 \text{ M}^{-1} \text{ s}^{-1}$) mostly reflects HAT from the methylene groups. On the basis of this observation, the ~ 5 -fold increase in k_{H} measured on going from PentH to PentOH clearly indicates that with the latter substrate HAT predominantly occurs from the CH_2 that is α to the OH group. Along the same line, the ~ 50 -fold increase in k_{H} measured on going from PentH to PentNH₂ and APOH indicates that with the latter two substrates HAT almost exclusively occurs from the CH_2 that is α to the NH₂ group, in full agreement with the results of previous studies on the reactions of alkylamines with alkoxy radicals.^{40c–e,46}

As compared to acetonitrile, when the reactions of CumO^\bullet with the same substrates have been studied in acetonitrile containing 0.2 M TFA, no significant effect on k_{H} has been observed for PentH, and a slight decrease in k_{H} has been measured for PentOH ($k_{\text{H}} = (1.08 \pm 0.03) \times 10^5 \text{ M}^{-1} \text{ s}^{-1}$, Figure S19), quantified on the basis of the rate constant ratio $k_{\text{H}}/k_{\text{H}}(\text{TFA}) = 1.35$. On the other hand, when the reaction of CumO^\bullet with PentNH₂ has been studied in the presence of TFA (0.1–1.0 M), no significant effect on reactivity has been observed up to $[\text{PentNH}_2] = [\text{TFA}]$ (Figure 4, region 1: black circles), indicating that in this concentration range, only an upper limit to k_{H} can be determined as $k_{\text{H1}} < 10^4 \text{ M}^{-1} \text{ s}^{-1}$.

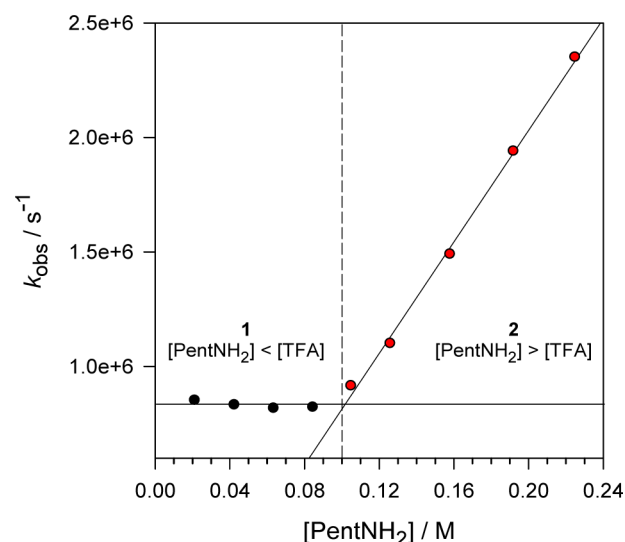
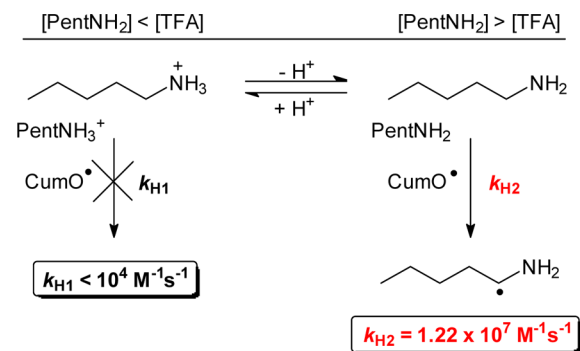


Figure 4. Plot of k_{obs} vs [pentylamine] for reaction with CumO^\bullet in MeCN containing 0.10 M TFA. From the linear regression analysis: for $[\text{PentNH}_2] \leq [\text{TFA}]$ (black circles), by taking into account that for $[\text{TFA}] = 0.1\text{--}1.0 \text{ M}$, no effect on k_{obs} has been observed up to $[\text{PentNH}_2] = [\text{TFA}]$, $k_{\text{H1}} < 10^4 \text{ M}^{-1} \text{ s}^{-1}$; for $[\text{PentNH}_2] > [\text{TFA}]$ (red circles) $k_{\text{H2}} = 1.22 \times 10^7 \text{ M}^{-1} \text{ s}^{-1}$.

Clearly, under these conditions protonation of the amine functionality strongly deactivates the α -C–H bonds (Scheme 8), leading to a decrease in reactivity that exceeds 3 orders of magnitude ($k_{\text{H}}/k_{\text{H}}(\text{TFA}) > 10^3$).

Scheme 8



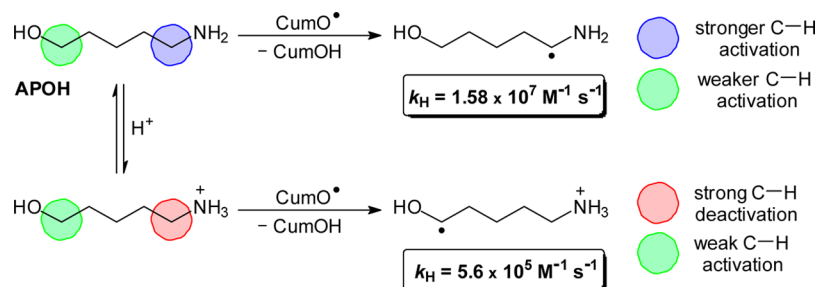
Most interestingly, comparison of this upper limit with the k_{H} value measured in acetonitrile for PentH ($k_{\text{H}} = 3.1 \times 10^5 \text{ M}^{-1} \text{ s}^{-1}$) shows that with PentNH₂, the strong deactivating polar effect determined by protonation extends up to the δ -methylene group, for which $k_{\text{H}}(\text{CH}_2) < 10^4 \text{ M}^{-1} \text{ s}^{-1}$.

For $[\text{PentNH}_2] > [\text{TFA}]$ a linear increase in k_{obs} with increasing $[\text{PentNH}_2]$ has been observed (Figure 4, region 2: red circles), leading to a rate constant value ($k_{\text{H2}} = 1.22 \times 10^7 \text{ M}^{-1} \text{ s}^{-1}$) that is very similar to the value measured in acetonitrile in the absence of TFA, indicating that in this concentration range HAT occurs from the α -C–H bonds of the nonprotonated amine (Scheme 8).

With APOH, in order to obtain information on the effect of TFA, the time-resolved kinetic study has been carried out by successive dilutions of an acetonitrile solution containing equimolar amounts of APOH and TFA (0.50 M).

The k_{obs} vs [substrate] plot for reaction of CumO^\bullet with APOH in the presence of TFA is displayed in Figure S20, from

Scheme 9



which $k_{\text{H}} = (5.6 \pm 0.1) \times 10^5 \text{ M}^{-1} \text{ s}^{-1}$ has been obtained. This value is 28 times lower than the value measured in acetonitrile in the absence of TFA, but, on the other hand, is at least 56 times higher than the upper limit determined for HAT from PentNH_3^+ to CumO^\bullet (Scheme 8). In keeping with the discussion outlined above, this behavior can be rationalized on the basis of Scheme 9, where protonation of the APOH amino group strongly deactivates the proximal and remote methylene groups toward HAT to CumO^\bullet .

However, differently than for PentNH_3^+ , where C–H deactivation has been shown to extend up to the δ -methylene group, the measured k_{H} value indicates that the presence of an OH group on the ε -carbon promotes selective HAT to CumO^\bullet from the C–H bonds that are adjacent to this functional group. The ~ 3 -fold decrease in k_{H} measured on going from PentOH to protonated APOH points nevertheless toward a deactivating polar effect of the remote NH_3^+ group on HAT from the C–H bonds that are α to the OH group.

CONCLUSIONS

Taken together, the results obtained in this study have clearly shown that in HAT reactions from the aliphatic C–H bonds of substrates bearing different functionalities or from the C–H bonds of substrates couples or triads characterized by different basicities, careful control over the site (intramolecular) and substrate (intermolecular) selectivity can be achieved through Brønsted and Lewis acid–base interactions, providing useful guidelines for the development of selective HAT-based C–H functionalization procedures. When dealing with bifunctional substrates, the results presented above indicate that site-selectivity can be drastically changed through protonation of a basic and strong activating NH_2 functionality over an OH one, with the latter group that directs HAT to the adjacent C–H bonds. In the intermolecular selectivity studies, the results for which are summarized in Table 2, the similar reactivity patterns observed after addition of TFA and $\text{Mg}(\text{ClO}_4)_2$, where protonation or Mg^{2+} binding strongly deactivates the C–H bonds of amine substrates toward HAT to CumO^\bullet , together with the observation that LiClO_4 promotes selective C–H bond deactivation of amide substrates, indicate that these additives can be employed in an orthogonal fashion for selective functionalization of hydrocarbon, ether, alcohol, and amide (or amine) substrates in the presence of an amine (or amide) one. These selectivity patterns are complemented by $\text{Ca}(\text{ClO}_4)_2$ that, by promoting, contemporarily, strong C–H bond deactivation for intrinsically activated amine and amide substrates, offers the opportunity to selectively functionalize alkane, ether, and alcohol substrates in the presence of the former ones.

EXPERIMENTAL SECTION

Materials. Spectroscopic grade acetonitrile was used in the kinetic experiments. The following substrates were of the highest commercial quality available and were used as received: cyclooctane (COT), dibenzylether (DBE), tetrahydrofuran (THF), cyclohexanol (CHXOH), *N,N*-dimethylacetamide (DMA), cyclohexylamine (CHXNH₂), triethylamine (TEA), 1,2,2,6,6-pentamethylpiperidine (PMP), pentane (PentH), 1-pentanol (PentOH), 1-aminopentane (PentNH₂), and 5-amino-1-pentanol (APOH).

Commercial samples of cumyl alcohol (CumOH), diacetoxyiodobenzene (DIB), and I₂ were used in the product studies. The reaction products observed in these studies were commercially available and were used as received (cyclooctylacetate (COTOAc), acetophenone (PhCOCH₃), benzaldehyde (PhCHO), and benzyl alcohol (PhCH₂OH)).

Dicumyl peroxide, trifluoroacetic acid (TFA), lithium perchlorate (LiClO_4), magnesium perchlorate ($\text{Mg}(\text{ClO}_4)_2$), and calcium perchlorate ($\text{Ca}(\text{ClO}_4)_2$) were of the highest commercial quality available and were used as received. Previous studies have shown the stability of dicumyl peroxide to TFA and to these perchlorate salts under the experimental conditions employed.^{33,34,37}

Laser Flash Photolysis (LFP) Studies. LFP experiments were carried out with a laser kinetic spectrometer using the third harmonic (355 nm) of a Q-switched Nd:YAG laser, delivering 8 ns pulses. The laser energy was adjusted to ≤ 10 mJ/pulse by the use of the appropriate filter. A 3.5 mL Suprasil quartz cell (10 mm \times 10 mm) was used in all experiments. Argon saturated acetonitrile solutions containing dicumyl peroxide (1.0 M) were employed. All the experiments were carried out at $T = 25 \pm 0.5$ °C under magnetic stirring. The observed rate constants (k_{obs}) were obtained by averaging 2–5 individual values and were reproducible to within 5%.

Second-order rate constant for the reactions of the cumyloxy radical with the different substrates were obtained from the slopes of the k_{obs} (measured following the decay of the cumyloxy radical visible absorption band at 490 nm) vs [substrate] plots. Transient kinetic studies on the reactions of CumO^\bullet with substrate couples and triads in the presence of [TFA] (between 0.10 and 1.00 M) or metal ion salts (LiClO_4 , $\text{Mg}(\text{ClO}_4)_2$ or $\text{Ca}(\text{ClO}_4)_2$; between 0.01 and 0.60 M) were carried out following different procedures: (a) addition of one substrate (hydrocarbon, ether, or alcohol) to an acetonitrile solution containing dicumyl peroxide, the Lewis or Brønsted acidic additive, and an amine, amide, or an amine + amide substrate couple; (b) sequential addition to an acetonitrile solution containing dicumyl peroxide of a first substrate (hydrocarbon, ether or alcohol), a second one (amine or amide), or a second and a third one (amine and amide), the acidic additive, and a second amount of the first substrate; (c) sequential addition to an acetonitrile solution containing dicumyl peroxide and the acidic additive of a first substrate (hydrocarbon, ether, or alcohol), a second one (amine or amide), or a second and a third one (amine and amide), and a second amount of the first substrate.

Product Studies. Product studies on the reactions of CumO^\bullet with COT and DBE were carried out following visible light irradiation ($\lambda_{\text{irr}} = 480$ nm, irradiation time = 30–120 min) of argon saturated dichloromethane solutions containing the substrate (0.2–1.0 M), cumyl alcohol (CumOH, 0.10 M), DIB (0.22 M), and I₂ (0.11 M).⁴⁵

In a typical experiment, 5 mL of an argon saturated dichloromethane solution containing the substrate, CumOH, DIB, and I₂, was introduced into a pyrex glass vessel equipped with an external jacket for water circulation. The reaction mixture was then irradiated with visible light at $T = 20\text{ }^{\circ}\text{C}$ employing a photochemical reactor equipped with $8 \times 15\text{ W}$ lamps. At the end of the irradiation, the solution was added to 10 mL of H₂O and then extracted with dichloromethane ($3 \times 10\text{ mL}$). The organic extracts were washed with a 10% sodium thiosulfate solution and dried over Na₂SO₄. All the preparation and workup procedures were carried out limiting exposure of the solution to light. Reaction products were identified by GC and GC-MS by comparison with authentic samples and quantified by GC employing 1,2-diphenylethane (bibenzyl) as internal standard. With both COT and DBE, no product formation was observed in the absence of irradiation by leaving the reaction mixtures in the dark for at least 1 h.

Reaction of CumO[•] with COT. When COT (5.0 mmol) and CumOH (0.50 mmol) were irradiated for 30 min in the presence of DIB (1.10 mmol) and I₂ (0.55 mmol), formation of COTOAc (0.09 mmol) and PhCOCH₃ (0.06 mmol) was observed. When the reaction of COT (2.0 mmol) was carried out under identical conditions in the presence of TFA (0.28 mmol) and PMP (0.27 mmol), formation of COTOAc (0.05 mmol) and PhCOCH₃ (0.12 mmol) was observed. PMP was recovered quantitatively (0.27 mmol) from the irradiated reaction mixture.

Reaction of CumO[•] with DBE. When DBE (1.0 mmol) and CumOH (0.50 mmol) were irradiated for 30 min in the presence of DIB (1.10 mmol) and I₂ (0.55 mmol), formation of PhCHO (0.34 mmol), PhCH₂OH (0.08 mmol) and PhCOCH₃ (0.14 mmol) was observed. When the same reaction was carried out in the presence of TFA (0.55 mmol) and PMP (0.50 mmol), formation of PhCHO (0.22 mmol), PhCH₂OH (0.06 mmol), and PhCOCH₃ (0.15 mmol) was observed. PMP was recovered quantitatively (0.49 mmol) from the irradiated reaction mixture.

■ ASSOCIATED CONTENT

📄 Supporting Information

The Supporting Information is available free of charge on the ACS Publications website at DOI: 10.1021/acs.joc.6b01842.

Plots of k_{obs} vs substrate concentration for the reactions of CumO[•] (PDF)

■ AUTHOR INFORMATION

Corresponding Author

*E-mail: bietti@uniroma2.it.

Notes

The authors declare no competing financial interest.

■ ACKNOWLEDGMENTS

Financial support from the Ministero dell'Istruzione dell'Università e della Ricerca (MIUR) project 2010PFLRJR (PRIN 2010-2011) is gratefully acknowledged. We thank Prof. Miquel Costas for helpful discussion and Prof. Lorenzo Stella for the use of a LFP equipment.

■ REFERENCES

- (1) (a) Hartwig, J. F.; Larsen, M. A. *ACS Cent. Sci.* **2016**, *2*, 281–292. (b) Hartwig, J. F. *J. Am. Chem. Soc.* **2016**, *138*, 2–24.
- (2) Davies, H. M. L.; Morton, D. J. *Org. Chem.* **2016**, *81*, 343–350.
- (3) White, M. C. *Science* **2012**, *335*, 807–809.
- (4) (a) Brückl, T.; Baxter, R. D.; Ishihara, Y.; Baran, P. S. *Acc. Chem. Res.* **2012**, *45*, 826–839. (b) Gutekunst, W. R.; Baran, P. S. *Chem. Soc. Rev.* **2011**, *40*, 1976–1991.
- (5) (a) Larsen, M. A.; Cho, S. H.; Hartwig, J. F. *J. Am. Chem. Soc.* **2016**, *138*, 762–765. (b) Larsen, M. A.; Wilson, C. V.; Hartwig, J. F. *J. Am. Chem. Soc.* **2015**, *137*, 8633–8643. (c) Li, Q.; Liskey, C. W.; Hartwig, J. F. *J. Am. Chem. Soc.* **2014**, *136*, 8755–8765. (d) Mkhaldid, I.

A. I.; Barnard, J. H.; Marder, T. B.; Murphy, J. M.; Hartwig, J. F. *Chem. Rev.* **2010**, *110*, 890–931.

(6) (a) Liao, K.; Negretti, S.; Musaev, D. G.; Bacsa, J.; Davies, H. M. L. *Nature* **2016**, *533*, 230–234. (b) Fu, L.; Guptill, D. M.; Davies, H. M. L. *J. Am. Chem. Soc.* **2016**, *138*, 5761–5764.

(7) Cook, A. K.; Schimler, S. D.; Matzger, A. J.; Sanford, M. S. *Science* **2016**, *351*, 1421–1424.

(8) Smith, K. T.; Berritt, S.; González-Moreias, M.; Ahn, S.; Smith, M. R., III; Baik, M.-H.; Mindiola, D. J. *Science* **2016**, *351*, 1424–1427.

(9) (a) Zhang, F.-L.; Hong, K.; Li, T.-J.; Park, H.; Yu, J.-Q. *Science* **2016**, *351*, 252–256. (b) Li, S.; Zhu, R.-Y.; Xiao, K.-J.; Yu, J.-Q. *Angew. Chem., Int. Ed.* **2016**, *55*, 4317–4321. (c) Jiang, H.; He, J.; Liu, T.; Yu, J.-Q. *J. Am. Chem. Soc.* **2016**, *138*, 2055–2059.

(10) (a) Topczewski, J. J.; Cabrera, P. J.; Saper, N. I.; Sanford, M. S. *Nature* **2016**, *531*, 220–224. (b) Neufeldt, S. R.; Sanford, M. S. *Acc. Chem. Res.* **2012**, *45*, 936–946. (c) Lyons, T. W.; Sanford, M. S. *Chem. Rev.* **2010**, *110*, 1147–1169.

(11) (a) Huang, Z.; Wang, C.; Dong, G. *Angew. Chem., Int. Ed.* **2016**, *55*, 5299–5303. (b) Ozawa, J.; Tashiro, M.; Ni, J.; Oisaki, K.; Kanai, M. *Chem. Sci.* **2016**, *7*, 1904–1909.

(12) Lewis, J. C.; Coelho, P. S.; Arnold, F. H. *Chem. Soc. Rev.* **2011**, *40*, 2003–2021.

(13) (a) Narayan, A. R. H.; Jiménez-Osés, G.; Liu, P.; Negretti, S.; Zhao, W.; Gilbert, M. M.; Ramabhadran, R. O.; Yang, Y.-F.; Furan, L. R.; Li, Z.; Podust, L. M.; Montgomery, J.; Houk, K. N.; Sherman, D. H. *Nat. Chem.* **2015**, *7*, 653–660. (b) Negretti, S.; Narayan, A. R. H.; Chiou, K. C.; Kells, P. M.; Stachowski, J. L.; Hansen, D. A.; Podust, L. M.; Montgomery, J.; Sherman, D. H. *J. Am. Chem. Soc.* **2014**, *136*, 4901–4904.

(14) (a) Roiban, G.-D.; Reetz, M. T. *Chem. Commun.* **2015**, *51*, 2208–2224. (b) Roiban, G.-D.; Agudo, R.; Reetz, M. T. *Angew. Chem., Int. Ed.* **2014**, *53*, 8659–8663. (c) Kille, S.; Zilly, F. E.; Acevedo, J. P.; Reetz, M. T. *Nat. Chem.* **2011**, *3*, 738–743.

(15) Rydzik, A. M.; Leung, I. K. H.; Kochan, G. T.; McDonough, M. A.; Claridge, T. D. W.; Schofield, C. J. *Angew. Chem., Int. Ed.* **2014**, *53*, 10925–10927.

(16) (a) Font, D.; Canta, M.; Milan, M.; Cussó, O.; Ribas, X.; Klein Gebbink, R. J. M.; Costas, M. *Angew. Chem., Int. Ed.* **2016**, *55*, 5776–5779. (b) Canta, M.; Font, D.; Gómez, L.; Ribas, X.; Costas, M. *Adv. Synth. Catal.* **2014**, *356*, 818–830. (c) Gómez, L.; Garcia-Bosch, I.; Company, A.; Benet-Buchholz, J.; Polo, A.; Sala, X.; Ribas, X.; Costas, M. *Angew. Chem., Int. Ed.* **2009**, *48*, 5720–5723.

(17) (a) Liu, W.; Groves, J. T. *Acc. Chem. Res.* **2015**, *48*, 1727–1735. (b) Huang, X.; Cheng, M.-J.; Nielsen, R. J.; Goddard, W. A., III; Groves, J. T. *J. Am. Chem. Soc.* **2015**, *137*, 5300–5303. (c) Liu, W.; Huang, X.; Cheng, M.-J.; Nielsen, R. J.; Goddard, W. A.; Groves, J. T. *Science* **2012**, *337*, 1322–1325.

(18) Ottenbacher, R. V.; Talsi, E. P.; Bryliakov, K. P. *ACS Catal.* **2015**, *5*, 39–44.

(19) (a) Gormisky, P. E.; White, M. C. *J. Am. Chem. Soc.* **2013**, *135*, 14052–14055. (b) Bigi, M. A.; Reed, S. A.; White, M. C. *J. Am. Chem. Soc.* **2012**, *134*, 9721–9726. (c) Chen, M. S.; White, M. C. *Science* **2007**, *318*, 783–787.

(20) Das, S.; Incarvito, C. D.; Crabtree, R. H.; Brudvig, G. W. *Science* **2006**, *312*, 1941–1943.

(21) Salamone, M.; Bietti, M. *Acc. Chem. Res.* **2015**, *48*, 2895–2903.

(22) (a) Zou, L.; Paton, R. S.; Eschenmoser, A.; Newhouse, T. R.; Baran, P. S.; Houk, K. N. *J. Org. Chem.* **2013**, *78*, 4037–4048. (b) Chen, K.; Eschenmoser, A.; Baran, P. S. *Angew. Chem., Int. Ed.* **2009**, *48*, 9705–9708. (c) Chen, K.; Baran, P. S. *Nature* **2009**, *459*, 824–828.

(23) Moteki, S. A.; Usui, A.; Zhang, T.; Solorio Alvarado, C. R.; Maruoka, K. *Angew. Chem., Int. Ed.* **2013**, *52*, 8657–8660.

(24) Newhouse, T.; Baran, P. S. *Angew. Chem., Int. Ed.* **2011**, *50*, 3362–3374.

(25) (a) Shaw, M. H.; Shurtleff, V. W.; Terrett, J. A.; Cuthbertson, J. D.; MacMillan, D. W. C. *Science* **2016**, *352*, 1304–1308. (b) Jeffrey, J. L.; Terrett, J. A.; MacMillan, D. W. C. *Science* **2015**, *349*, 1532–1536.

(26) (a) Quinn, R. K.; Könst, Z. A.; Michalak, S. E.; Schmidt, Y.; Szklarski, A. R.; Flores, A. R.; Nam, S.; Horne, D. A.; Vanderwal, C. D.; Alexanian, E. J. *J. Am. Chem. Soc.* **2016**, *138*, 696–702. (b) Schmidt, V. A.; Quinn, R. K.; Brusoe, A. T.; Alexanian, E. J. *J. Am. Chem. Soc.* **2014**, *136*, 14389–14392.

(27) Sharma, A.; Hartwig, J. F. *Nature* **2015**, *517*, 600–604.

(28) Roberts, B. P. *Chem. Soc. Rev.* **1999**, *28*, 25–35.

(29) Howell, J. M.; Feng, K.; Clark, J. R.; Trzepakowski, L. J.; White, M. C. *J. Am. Chem. Soc.* **2015**, *137*, 14590–14593.

(30) Adams, A. M.; Du Bois, J.; Malik, H. A. *Org. Lett.* **2015**, *17*, 6066–6069.

(31) Asensio, G.; González-Núñez, M. E.; Bernardini, C. B.; Mello, R.; Adam, W. J. *J. Am. Chem. Soc.* **1993**, *115*, 7250–7253.

(32) An analogous selectivity has been also observed in the Fe-catalyzed oxyfunctionalization and Pt-catalyzed oxidation of aliphatic amines following substrate protonation, see: (a) Mbofana, C. T.; Chong, E.; Lawniczak, J.; Sanford, M. S. *Org. Lett.* **2016**, *18*, 4258–4261. (b) Lee, M.; Sanford, M. S. *J. Am. Chem. Soc.* **2015**, *137*, 12796–12799.

(33) Salamone, M.; Mangiacapra, L.; DiLabio, G. A.; Bietti, M. *J. Am. Chem. Soc.* **2013**, *135*, 415–423.

(34) (a) Milan, M.; Salamone, M.; Bietti, M. *J. Org. Chem.* **2014**, *79*, 5710–5716. (b) Salamone, M.; Giammarioli, I.; Bietti, M. *Chem. Sci.* **2013**, *4*, 3255–3262.

(35) Nova, A.; Balcells, D. *Chem. Commun.* **2014**, *50*, 614–616.

(36) Transient kinetic studies have shown that in HAT to CumO[•], the addition of Ca(ClO₄)₂ leads to strong C–H bond deactivation for tertiary amine substrates such as triethylamine (TEA) and 1,2,2,6,6-pentamethylpiperidine (PMP) up to [Ca²⁺] ≤ [substrate]. See, for example, Figure S21 showing the effect of Ca(ClO₄)₂ on the reaction of CumO[•] with PMP.

(37) (a) Salamone, M.; Carboni, G.; Mangiacapra, L.; Bietti, M. *J. Org. Chem.* **2015**, *80*, 9214–9223. (b) Salamone, M.; Mangiacapra, L.; Carboni, G.; Bietti, M. *Tetrahedron* ASAP. DOI: 10.1016/j.tet.2016.05.047.

(38) For a critical discussion and a quantitative evaluation of the role of polar effects on the kinetics and thermodynamics of HAT from aliphatic C–H bonds, see: (a) Chan, B.; Easton, C. J.; Radom, L. *J. Phys. Chem. A* **2015**, *119*, 3843–3847. (b) Amos, R. I. J.; Chan, B.; Easton, C. J.; Radom, L. *J. Phys. Chem. B* **2015**, *119*, 783–788. (c) O'Reilly, R. J.; Chan, B.; Taylor, M. S.; Ivanic, S.; Bacskay, G. B.; Easton, C. J.; Radom, L. *J. Am. Chem. Soc.* **2011**, *133*, 16553–16559.

(39) (a) Baciocchi, E.; Bietti, M.; Salamone, M.; Steenken, S. *J. Org. Chem.* **2002**, *67*, 2266–2270. (b) Avila, D. V.; Ingold, K. U.; Di Nardo, A. A.; Zerbetto, F.; Zgierski, M. Z.; Luszytk, J. *J. Am. Chem. Soc.* **1995**, *117*, 2711–2718.

(40) (a) Malatesta, V.; Scaiano, J. C. *J. Org. Chem.* **1982**, *47*, 1455–1459. (b) Paul, H.; Small, R. D., Jr.; Scaiano, J. C. *J. Am. Chem. Soc.* **1978**, *100*, 4520–4527. (c) Finn, M.; Friedline, R.; Suleman, N. K.; Wohl, C. J.; Tanko, J. M. *J. Am. Chem. Soc.* **2004**, *126*, 7578–7584. (d) Salamone, M.; DiLabio, G. A.; Bietti, M. *J. Am. Chem. Soc.* **2011**, *133*, 16625–16634. (e) Pischel, U.; Nau, W. M. *J. Am. Chem. Soc.* **2001**, *123*, 9727–9737.

(41) Salamone, M.; Milan, M.; DiLabio, G. A.; Bietti, M. *J. Org. Chem.* **2013**, *78*, 5909–5917.

(42) Bietti, M.; Martella, R.; Salamone, M. *Org. Lett.* **2011**, *13*, 6110–6113.

(43) Suárez, E.; Rodríguez, M. S. In *Radicals in Organic Synthesis*; Renaud, P., Sibi, M. P., Eds.; Wiley-VCH: Weinheim, 2001; Vol. 2, pp 440–454.

(44) The time course of the decay of absorbance at 490 nm for the reaction of CumO[•] with COT in MeCN and in MeCN containing 0.01 M PMP, 0.2 M DMA, and 0.2 M Ca(ClO₄)₂ is displayed in Figure S2.

(45) (a) Weber, M.; Fischer, H. *J. Am. Chem. Soc.* **1999**, *121*, 7381–7388. (b) Salamone, M.; Basili, F.; Mele, R.; Cianfanelli, M.; Bietti, M. *Org. Lett.* **2014**, *16*, 6444–6447.

(46) HAT from the O–H and N–H bonds of PentOH, PentNH₂, and APOH can be ruled on the basis of the significantly higher BDE of

the former bonds as compared to the C–H bonds that are α to the OH and NH₂ groups and of the significantly lower k_{H} values measured previously for HAT from the OH group of alcohols and the NH₂ group of alkylamines to tertiary alkoxy radicals (refs 40d, 40e, and 47).

(47) Griller, D.; Ingold, K. U. *J. Am. Chem. Soc.* **1974**, *96*, 630–632.